Operating Point Setting Method for Wireless Power Transfer with Constant Voltage Load

Daisuke Gunji
The University of Tokyo / NSK Ltd.
5-1-5, Kashiwanoha, Kashiwa, Chiba, 277-8561, Japan
/ 1-5-50, Kugenumashinmei, Fujisawa,
Kanagawa, 251-8501, Japan
Email: gunji@hflab.k.u-tokyo.ac.jp

Takehiro Imura and Hiroshi Fujimoto
The University of Tokyo
5-1-5, Kashiwanoha, Kashiwa, Chiba, 277-8561, Japan
Phone: +81-4-7136-3881
Email:imura@hori.k.u-tokyo.ac.jp
fujimoto@k.u-tokyo.ac.jp

***Abstract*—Wireless Power Transfer (WPT) has been widely researched in many application fields. Typical application to vehicle field is wireless charging for electric vehicles while parking and driving. Some power conversion circuit structures and its control method have been proposed in previous researches, for example, transmitting power control and efficiency maximizing control using a secondary-side DC-DC converter. However, selection method of optimal circuit structure for desired control is not clear. In this research, we propose generalized power conversion circuit structure on Series-Series compensated WPT circuit. Load current and power transfer efficiency are analyzed using equivalent AC resistance model about WPT circuit with constant voltage load. Then, we formulate operation points for desired control with consideration for operating condition.**

I. Introduction

Wireless Power Transfer (WPT) via magnetic resonance coupling [1] has recently received broad attention. As application to vehicle field, many previous researches have been reported about wireless battery charging for electric vehicles while parking [2], [3] and while driving [4], [5]. Our research group has proposed Wireless In-Wheel Motor which can improve reliability and safety of an In-Wheel Motor by using bidirectional wireless power transfer system [6].

In order to control of transmitting power and efficiency, power conversion circuit is necessary on WPT circuit. Many circuit structures have been proposed on previous researches. In order to improve power transfer efficiency, many previous researches have been proposed efficiency optimization control method by manipulating equivalent load resistance using secondary-side DC-DC converter [8]–[10]. Also, by using secondary-side DC-DC converter, transmitting power control for constant voltage load has been proposed [11]. To realize bidirectional power transfer for Vehicle to Grid application, it has been proposed that using full bridge switching circuits both primary-side and secondary side [7]. In the case of the W-IWM, a secondary-side converter is used not only for bidirectional power transfer but for transmitting power control on powering state [6]. However, selection method of power conversion circuit for desired control is not clear. In addition, operating point setting considering power conversion circuit structure is not formulated.

In this research, we propose generalized power conversion circuit structure of Series-Series (SS) compensated WPT circuit via magnetic resonance coupling with constant voltage load. We formulate operating points of primary-side and secondary-side power conversion circuit on five operating conditions. These formulae are useful not only for control of power conversion circuits, but for power conversion circuits structure design. The usefulness of these formulae are verified by experiments.

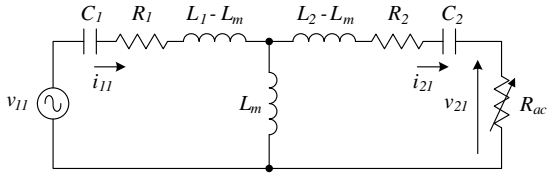

Fig. 1. AC circuit model.

II. AC circuit analysis

A. AC circuit model

In order to analyze transmitting power and efficiency, AC circuit model is introduced as equivalent model of WPT circuit include power conversion circuit. The model is shown in Fig. 1. It is possible to apply analysis results of SS compensated WPT circuit with AC resistive road [13] to the circuit including power conversion circuits by using the AC model. On the model, the primary-side and the secondary-side LC circuit is expressed with T-type equivalent circuit [14]. In addition, equivalent AC resistance R_{ac} is introduced. R_{ac} is equivalent variable resistance which varies with operation of power conversion circuits. R_{ac} is defined as follows:

$$R_{ac} = \frac{V_{21}}{I_{21}}, \tag{1}$$

where V_{21} and I_{21} are respectively RMS value of the fundamental wave component of a secondary AC-DC conversion circuit input voltage v_{21} and current i_{21}. In this research, we assume that $i_{21} = i_2$ and resonant condition is satisfied. The primary voltage source v_{11} in the AC model is fundamental wave component of output voltage of a primary inverter.

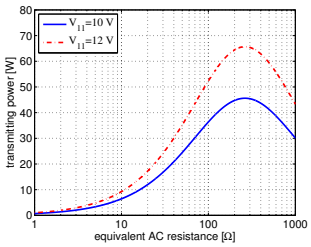

(a) R_{ac} vs. power.

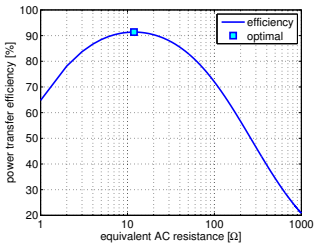

(b) R_{ac} vs. efficiency.

Fig. 2. Power transfer characteristics.

B. Transmitting power

According to circuit equation of the AC model, electric power of R_{ac} is expressed as follows:

$$P_R = \frac{(\omega_0 L_m)^2 R_{ac}}{\left\{R_1 R_2 + R_1 R_{ac} + (\omega_0 L_m)^2\right\}^2} {V_{11}}^2, \quad (2)$$

where ω_0 is resonant angular frequency, L_m is mutual inductance between coils, R_1 and R_2 are respectively internal resistance of the primary coil and the secondary coil, C_1 and C_2 are respectively resonant capacitor of the primary-side and the secondary-side. According to eq. (2), transmitting power is manipulated by V_{11} and R_{ac}, where V_{11} is RMS value of v_{11}. If we ignore electric losses on secondary-side power conversion circuits, P_R is equal to a load power. Fig. 2(a) shows transmitting power characteristics with V_{11} and R_{ac}. Circuit parameters are listed in TABLE IV.

C. Power transfer efficiency

Power transfer efficiency η is also calculated from circuit equation of the AC model as follows:

$$\eta = \frac{(\omega_0 L_m)^2 R_{ac}}{(R_2+R_{ac})\left\{R_1 R_2+R_1 R_{ac}+(\omega_0 L_m)^2\right\}}. \quad (3)$$

According to eq. (3), power transfer efficiency is decided only in R_{ac} regardless of V_{11}. The optimal equivalent resistance $R_{\eta opt}$ which maximize power transfer efficiency is derived from eq. (3) as follows:

$$R_{\eta opt} = \sqrt{\frac{R_2}{R_1}(\omega_0 L_m)^2 + {R_2}^2}. \quad (4)$$

Fig. 2(b) shows efficiency characteristics.

D. Control degree-of-freedom

According to eq. (2) and eq. (3), manipulated variables are only V_{11} and R_{ac} for transmitting power and efficiency control if we ignore electrical losses of power conversion circuits. V_{11} is manipulated by using a primary DC-AC conversion circuit. R_{ac} is manipulated by using secondary-side power conversion circuits. Therefore, if we want to control both V_{11} and R_{ac}, at least one controllable power conversion circuit is respectively required both primary-side and secondary-side.

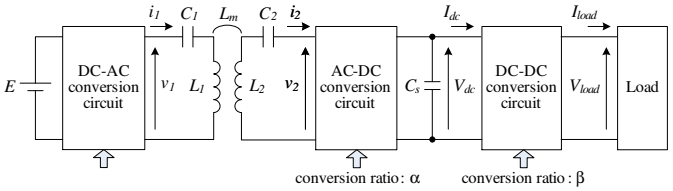

Fig. 3. Generalized SS compensated WPT circuit.

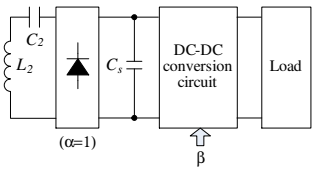

(a) Using diode bridge rectifier.

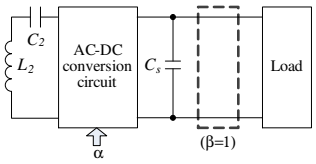

(b) Without DC-DC converter.

Fig. 4. Special example of secondary circuit.

III. Generalization of Power Conversion Circuits

A. Generalized circuit structure

We introduce generalized circuit structure of SS compensated WPT circuit with power conversion circuits as shown in Fig. 3. The primary side consists of DC voltage source, DC-AC conversion circuit (describe it as primary inverter), and resonator LC circuit. The primary inverter generates high frequency electricity and also controls V_{11}.

High frequency electricity is transmitted to the secondary side via magnetic resonance coupling. Received power is rectified by the secondary AC-DC converter. DC-link voltage and current is controlled by the secondary DC-DC converter. Then, transmitted power is supplied to a load.

As shown in Fig. 4 (a) and (b), using diode bridge rectifier on the secondary AC-DC converter and without secondary DC-DC converter are special example of the generalized circuit. Therefor we can handle that circuit with the same framework by the generalized circuit structure.

B. Primary-side AC-DC conversion circuit

There are two options of primary-side power conversion circuit structure. One is PWM method which controls V_{11} by operating pulse width of the primary inverter. Another option is PAM method which is using buck-boost DC-DC converter and fixed pulse width inverter. Both two circuit structure have same function from the point of view of control of V_{11}.

C. Definition of conversion ratio

We introduce conversion ratio of secondary-side power conversion circuit. On the circuit shown in Fig. 3, we ignore losses on each power conversion circuit and assume that power factor of fundamental wave component on the secondary AC-DC conversion circuit input is 1. Then, relations between input and output are expressed as following formulae:

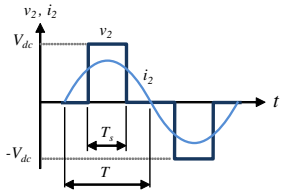

Fig. 5. Synchronous PWM rectification method.

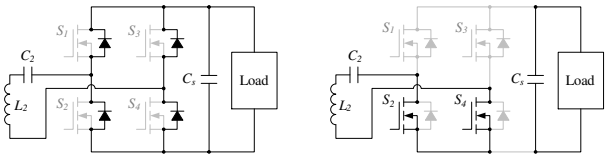

(a) Rectification mode. (b) Short mode.

Fig. 6. Operation modes of the secondary converter.

$$I_{dc} = \frac{2\sqrt{2}}{\pi}\alpha I_{21}, \quad (5)$$

$$V_{dc} = \frac{\pi}{2\sqrt{2}}\frac{1}{\alpha}V_{21}, \quad (6)$$

$$I_{load} = \beta I_{dc}, \quad (7)$$

$$V_{load} = \frac{1}{\beta}V_{dc}, \quad (8)$$

where α is current conversion ratio of the secondary-side AC-DC conversion circuit, and β is current conversion ratio of the secondary-side DC-DC conversion circuit. From eq. (5) to eq. (8), following equation is derived about R_{ac}.

$$R_{ac} = \frac{V_{21}}{I_{21}} = \frac{8}{\pi^2}(\alpha\beta)^2\frac{V_{load}}{I_{load}}, \quad (9)$$

where V_{load} and I_{load} are respectively load voltage and current. Then, $R_{load} = V_{load}/I_{load}$ means equivalent load resistance. We define total conversion ratio γ as follows:

$$\gamma = \alpha\beta. \quad (10)$$

By substituting eq. (10) into eq. (9), the following equation is derived.

$$R_{ac} = \frac{8}{\pi^2}\gamma^2 R_{load}. \quad (11)$$

Eq. (11) suggests that conversion from R_{load} to R_{ac} can be controlled by γ.

D. Secondary-side AC-DC conversion circuit

Secondary-side AC-DC conversion circuit is full-bridge circuit same as voltage type single phase PWM converter. There are two operation methods. One is synchronous PWM rectification method [6]. In this method, switches are operated synchronously with the secondary current i_2 as shown in Fig. 5. The conversion ratio α is related with PWM duty ratio.

Another operation method is two mode method [12]. In this method, both lower arm switching devices are switched as shown in Fig. 6 (a) and (b). Fig. 6 (a) shows rectification mode. In this mode, electric power is transmitted from primary-side to the load. On the other hand, on the short mode as shown in Fig. 6 (b), electric power is not transmitted because the secondary-side circuit is shorted. By changing these two operation mode, transmitting power can be controlled. Therefore, the conversion ratio α is related with time ratio of above two operation modes.

Operation range of α is $0 \leq \alpha \leq 1$ regardless of operation method. Then R_{ac} is kept or decreased by operation of α. If AC-DC conversion circuit is diode bridge circuit, $\alpha = 1$.

TABLE I
OPERATING RANGE OF β.

Type	Voltage	β	R_{ac}
Buck	$V_{dc} > V_{load}$	$1 < \beta < \beta_{max}$	increase
Boost	$V_{dc} < V_{load}$	$\beta_{min} < \beta < 1$	decrease
Buck-boost	both	$\beta_{min} < \beta < \beta_{max}$	both

TABLE II
COMBINATION OF POWER CONVERSION CIRCUITS.

type	AC-DC	DC-DC	$\gamma = \alpha\beta$
A	Converter	Buck	$0 \leq \gamma < \beta_{max}$
B		Boost	$0 \leq \gamma \leq 1$
C		Buck-boost	$0 \leq \gamma < \beta_{max}$
D		None	$0 \leq \gamma \leq 1$
E	Rectifier	Buck	$1 < \gamma < \beta_{max}$
F		Boost	$\beta_{min} < \gamma < 1$
G		Buck-boost	$\beta_{min} < \gamma < \beta_{max}$
H		None	1

E. DC-DC conversion circuit

Secondary-side DC-DC conversion circuit is connected to the output of the AC-DC conversion circuit in series. We assume that the load-side is the output of the DC-DC converter. From eq. (7) and eq. (8), operation range of β are expressed as shown in TABLE I.

According to eq. (9), R_{ac} is increased by using a buck type DC-DC converter. On the other hand, R_{ac} is decreased by using a boost type DC-DC converter. If there are no DC-DC converter, we can treat it as $\beta = 1$.

F. Combination of secondary-side power conversion circuit

Total conversion ratio γ which depends on combination of secondary-side power conversion circuits are listed in TABLE II. Type A structure achieves wide range of γ. In addition, bidirectional power transfer is available if buck DC-DC converter is a bidirectional chopper. Type B and C are undesirable structure because function of the AC-DC converter and boost type DC-DC converter are duplicative.

IV. OPERATING POINT SETTING METHOD

In this section, we propose operating point setting method of wireless power transfer for a constant voltage load on following five operating conditions.

- **CASE A:** Primary voltage is fixed, load current control
- **CASE B:** Primary voltage is fixed, maximum efficiency control
- **CASE C:** γ is fixed to 1, load current control
- **CASE D:** γ is fixed to 1, maximum efficiency control
- **CASE E:** Simultaneous control of load current and maximum efficiency

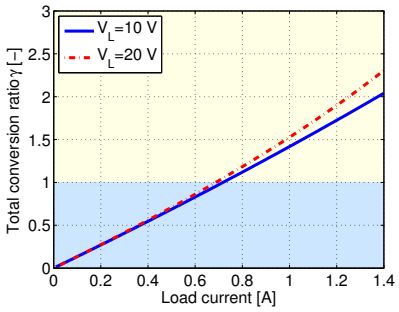

Fig. 7. I_L^* vs. γ on CASE A.

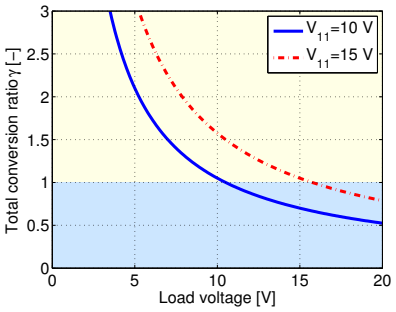

Fig. 8. V_L vs. γ on CASE B.

A. CASE A

For example, on dynamic wireless charging for EVs, it is preferred that primary voltage is fixed due to simplify primary-side equipment. In that case, we can control either transmitting power or efficiency, but not both because manipulated variable is only R_{ac}. On the CASE A, control target is load current, then power transfer efficiency is decided dependently.

From eq. (2) and eq. (11), total conversion ratio γ which can realize required load current I_L^* are calculated by the following formula:

$$\gamma = \frac{A \pm \sqrt{A^2 - \frac{\pi^2}{2}\frac{I_L^*}{R_1 V_L}\left\{R_1R_2 + (\omega_0 L_m)^2\right\}}}{2}, \quad (12)$$

$$A = \frac{\pi}{2\sqrt{2}}\frac{\omega_0 L_m V_{11}}{R_1 V_L},$$

where V_L is load voltage. As shown in Fig. 2 (a), there are two operating points which can realize I_L^*. Smaller γ of a solution for eq. (12) is a good option because it can realize higher efficiency than another solution. Fig. 7 shows relation between I_L^* and γ when V_{11} is 10 V and V_L is 10 or 20 V. According to Fig. 7, for example, if desired I_L^* is 0.2 to 1.4, required γ changes from less than one to over one. That means we have to select secondary-side power conversion circuit structure to satisfy such required operation range of γ.

B. CASE B

In the CASE B, target is power transfer efficiency maximization. The load current is decided dependently. From eq. (2) and eq. (11), γ which realize maximum efficiency is calculated by the following formula:

$$\gamma = \frac{\pi}{2\sqrt{2}}\frac{\omega_0 L_m R_{\eta opt}}{R_1R_2 + R_1R_{\eta opt} + (\omega_0 L_m)^2}\frac{V_{11}}{V_L}. \quad (13)$$

Calculation result is shown in Fig. 8. Required γ decrease as the load voltage V_L increase because equivalent load resistance increase with increase in V_L.

C. CASE C

The simplest structure of secondary-side is only using diode rectifier. In that case, conversion ratio is $\alpha = \beta = \gamma = 1$ and it is impossible to manipulate R_{ac} on secondary-side. Load current I_L is calculated by the following formula:

$$I_L = \frac{2\sqrt{2}}{\pi}\frac{\omega_0 L_m V_{11} - \frac{2\sqrt{2}}{\pi}R_1 V_L}{R_1R_2 + (\omega_0 L_m)^2}. \quad (14)$$

Therefore, primary voltage V_{11} which realize desired load current I_L^* is calculated by the following formula:

$$V_{11} = \frac{2\sqrt{2}}{\pi}\frac{R_1 V_L}{\omega_0 L_m} + \frac{\pi}{2\sqrt{2}}\frac{R_1R_2 + (\omega_0 L_m)^2}{\omega_0 L_m}I_L^*. \quad (15)$$

According to eq. (15), required V_{11} is proportional to I_L^*.

D. CASE D

If conversion ratio is $\alpha = \beta = \gamma = 1$, equivalent AC resistance R_{ac} is calculated as following formula:

$$R_{ac} = \frac{2\sqrt{2}}{\pi}\frac{R_1R_2 + (\omega_0 L_m)^2}{\omega_0 L_m V_{11} - \frac{2\sqrt{2}}{\pi}R_1 V_L}V_L. \quad (16)$$

Denominator of eq. (16) includes V_{11}, that means R_{ac} changes with V_{11} in the case of a constant voltage load. Therefore, V_{11} which realize maximum power transfer efficiency is derived from eq. (16) as following formula:

$$V_{11} = \frac{2\sqrt{2}}{\pi}\frac{R_1R_2 + R_1V_L + (\omega_0 L_m)^2}{\omega_0 L_m R_{\eta opt}}V_L. \quad (17)$$

Load current I_L is calculated by eq. (14).

E. CASE E

If both V_{11} and R_{ac} are controllable in a coordinated manner, operating point of V_{11} and γ which can realize both desired load current I_L^* and maximum power transfer efficiency are expressed as following formulae:

$$V_{11} = \frac{R_1R_2 + R_1R_{\eta opt} + (\omega_0 L_m)^2}{\omega_0 L_m}\sqrt{\frac{V_L}{R_{\eta opt}}}I_L^*, \quad (18)$$

$$\gamma = \frac{\pi}{2\sqrt{2}}\sqrt{\frac{R_{\eta opt}}{V_L}}I_L^*. \quad (19)$$

Fig. 9 (a) shows relation between I_L^* and V_{11}, and Fig. 9 (b) shows relation between I_L^* and γ when load voltage V_L is 10 or 20 V. Required V_{11} increase with increasing I_L^* and V_L. On the other hand, required γ decrease with increasing V_L because R_{load} increase with increasing V_L.

Operating point of V_{11} and γ on each case are listed in TABLE III.

TABLE III
OPERATING POINT ON CONSTANT VOLTAGE LOAD

CASE	Controlled variable		Manipulated variable	
	I_L	Efficiency	V_{11}	γ
A	desired	dependent	fixed	$\frac{\frac{\pi}{2\sqrt{2}}\frac{\omega_0 L_m V_{11}}{R_1 V_L} \pm \sqrt{\frac{\pi^2}{8}\left(\frac{\omega_0 L_m V_{11}}{R_1 V_L}\right)^2 - \frac{\pi^2}{2}\frac{I_L^*}{R_1 V_L}\left\{R_1 R_2 + (\omega_0 L_m)^2\right\}}}{2}$
B	dependent	maximized	fixed	$\frac{\pi}{2\sqrt{2}}\frac{\omega_0 L_m R_{\eta opt}}{R_1 R_2 + R_1 R_{\eta opt} + (\omega_0 L_m)^2}\frac{V_{11}}{V_L}$
C	desired	dependent	$\frac{2\sqrt{2}}{\pi}\frac{R_1 V_L}{\omega_0 L_m} + \frac{\pi}{2\sqrt{2}}\frac{R_1 R_2 + (\omega_0 L_m)^2}{\omega_0 L_m} I_L^*$	1
D	dependent	maximized	$\frac{2\sqrt{2}}{\pi}\frac{R_1 R_2 + R_1 V_L + (\omega_0 L_m)^2}{\omega_0 L_m R_{\eta opt}} V_L$	1
E	desired	maximized	$\frac{R_1 R_2 + R_1 R_{\eta opt} + (\omega_0 L_m)^2}{\omega_0 L_m}\sqrt{\frac{V_L}{R_{\eta opt}}} I_L^*$	$\frac{\pi}{2\sqrt{2}}\sqrt{\frac{R_{\eta opt}}{V_L}} I_L^*$

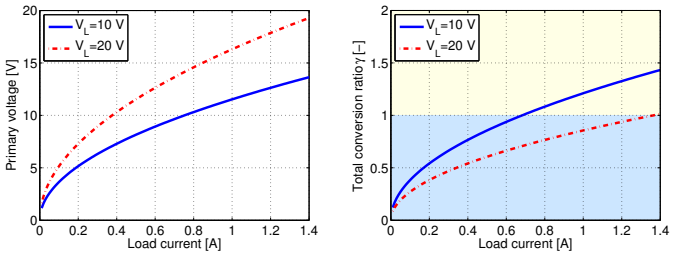

(a) I_L^* vs. V_{11}. (b) I_L^* vs. γ.

Fig. 9. Operating point on CASE E.

V. EXPERIMENT

A. Experimental equipment

Experimental equipment is shown in Fig. 10 (a). Circuit of the equipment is shown in Fig. 10 (b). The equipment consists of a DC power supply, a primary inverter, primary and secondary coils, a secondary AC-DC converter, a secondary DC-DC buck converter, an electric load (PLZ1004W: KIKUSUI), and a DPS (DS1104: dSPACE). Circuit parameters are listed in TABLE IV. Both conversion ratio α and β are controlled by the DSP. Primary voltage is manipulated by changing DC supply voltage E. DC source current is measured by monitor value of the DC power supply. Load current is measured by monitor value of the electric load. Total conversion ratio γ is distributed to α and β in accordance with follows:

- $\gamma \leq 1.05$: $\alpha = \gamma/1.05$, $\beta = 1.05$
  (due to operation of gate driver on the DC-DC converter)
- $1.05 < \gamma$: $\alpha = 1.00$, $\beta = \gamma$

B. CASE A

Experiment have been carried out on operating condition CASE A. Primary voltage V_{11} was set to 10 V. Load voltage V_L was set to 10 V. Primary-side DC power is calculated from DC source voltage E and DC source current. Load power is calculated as $V_L I_L$. Therefore, measured efficiency is DC to DC efficiency. We set total conversion ratio γ from 0.1 to 2.0 every 0.1.

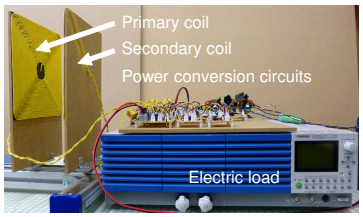

(a) Overview.

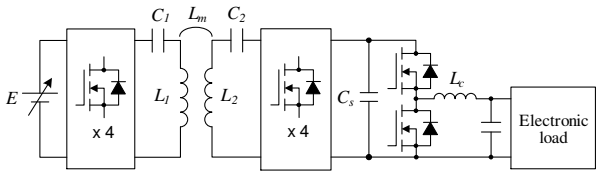

(b) Circuit structure.

Fig. 10. Experimental equipment.

TABLE IV
SPECIFICATIONS OF CIRCUIT

	Primary	Secondary
Coil resistance $R_{1,2}$	0.547 Ω	0.535 Ω
Coil inductance $L_{1,2}$	166 μH	167 μH
Capacitance $C_{1,2}$	19.9 nF	19.9 nF
Coil size	200 x 200 mm	
Coil gap	100 mm	
Mutual inductance L_m	21.8 μH	
Resonance frequency	87.6 kHz	
Smoothing capacitor C_s	1000 μF	
Reactor of DC-DC converter L_c	1.1 mH	

Experimental results are shown in Fig. 11. Fig. 11 (a) shows measurement result of I_L versus γ. Measurement result is in good accordance with calculation by eq. (12). Fig. 11 (b) and (c) respectively show I_L versus R_{ac} and I_L versus power transfer efficiency. R_{ac} is calculated from measured load voltage and current and γ by eq. (11). Absolute values of the efficiency are different between calculated value and experimental results because calculated values do not contain power losses of power conversion circuits. However, a similar tendency is seen in the change of efficiency for I_L. From these experimental results, the effectiveness of analysis method using R_{ac} and γ is verified.

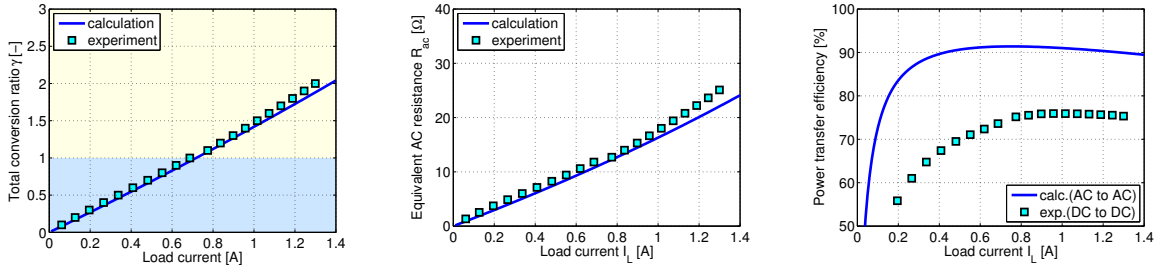

(a) I_L vs. γ. (b) I_L vs. R_{ac}. (c) I_L vs. efficiency.

Fig. 11. Experimental result of CASE A.

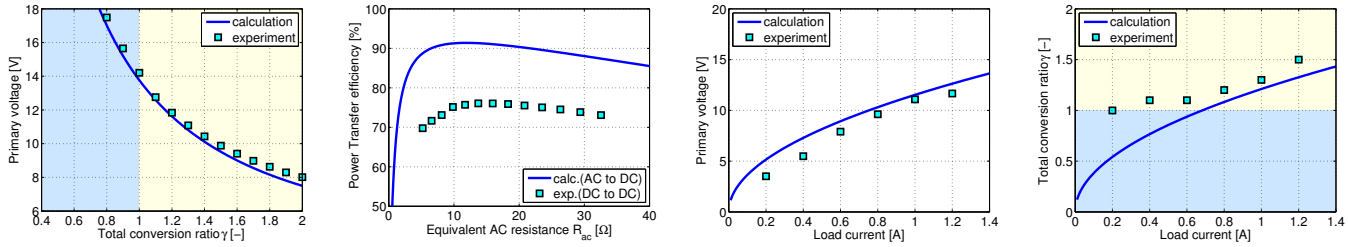

(a) γ vs. V_{11} ($I_L = 1.0$ A). (b) R_{ac} vs. η ($I_L = 1.0$ A). (c) I_L vs. optimized V_{11}. (d) I_L vs. optimized γ.

Fig. 12. Experimental result of CASE E.

C. CASE E

We also did a experiment about operating condition CASE E. We set γ from 0.1 to 2.0 every 0.1 and adjusted V_{11} to I_L becomes desired value, and then get optimized operating points (V_{11}, γ) on every 0.2 A of I_L from 0.2 A to 1.2 A.

Experimental results are shown in Fig. 12. Fig. 12 (a) shows operating points variation and Fig. 12 (b) shows measured efficiency of each operating points on $I_L = 1.0$ A. Fig. 12 (c) and (d) respectively show optimized V_{11} and γ. Similar tendency are seen in the change of optimized V_{11} and γ for R_{ac} between calculated value and experimental result. From these experimental results, the usefulness of the proposed operating point setting method is verified. Difference between calculation and experiment is due to electric power loss of power conversion circuits. Especially, error becomes bigger when γ is small due to loss on the short mode operation.

VI. Conclusion

In this research, we propose generalized power conversion circuit structure of SS compensated WPT circuit with constant voltage load. We formulate operating point of V_{11} and total conversion ratio γ on five operating conditions. Future works are considering electric loss on power conversion circuit and distribution method of γ to α and β.

References

[1] A. Kurs, A. Karalis, R. Moffatt, J. D. Joannopoulos, P. Fisher, M. Soljacic, "Wireless Power Transfer via Strongly Coupled Magnetic Resonances", Science Expression on 7 June 2007, Vol. 317, No. 5834, pp. 83–86 (2007)

[2] Y. Nagatsuka, N. Ehara, Y. Kaneko, S. Abe, and T. Yasuda: "Compact contactless power transfer system for electric vehicles ", Proc. IPEC 2010, pp. 807–813 (2010)

[3] M. Budhia, J. T. Boys, G. A. Covic, and Chang-Yu Huang: "Development of a Single-Sided Flux Magnetic Coupler for Electric Vehicle IPT Charging Systems", IEEE Trans. Industrial Electronics, Vol. 60, No. 1, pp. 318–328 (2013)

[4] J. Shin, S. Shin, Y. Kim, S. Ahn, S. Lee, G. J, S. Jeon, and D. Cho: "Design and Implementation of Shaped Magnetic-Resonance-Based Wireless Power Transfer System for Roadway-Powered Moving Electric Vehicles", IEEE Trans. Industrial Electronics, Vol. 61, No. 3, pp. 1179–1192 (2014)

[5] K. Throngnumchai, A. Hanamura, Y. Naruse, and K. Takeda: "Design and evaluation of a wireless power transfer system with road embedded transmitter coils for dynamic charging of electric vehicles", Proc. EVS27, pp. 1–10 (2013)

[6] D. Gunji, T. Imura, and H. Fujimoto: "Fundamental Research of Power Conversion Circuit Control for Wireless In-wheel Motor using Magnetic Resonance Coupling", Proc. IECON 2014, pp. 3004–3009 (2014)

[7] U. K. Madawala, and D. J. Thrimawithana: "A Bidirectional Inductive Power Interface for Electric Vehicle in V2G Systems", IEEE Trans. Industrial Electronics, Vol. 58, No. 10, pp. 4789–4796 (2011)

[8] H. Ishihara, F. Moritsuka, H. Kudo, S. Obayashi, T. Itakura, A. Matsushita, H. Mochikawa, and S. Otaka: "A Voltage Ratio-based Efficiency Control Method for 3 kW Wireless Power Transmission", Proc. APEC 2014, pp. 1312–1316 (2014)

[9] M. Fu, C. Ma, and X. Zhu: "A Cascaded Boost-Buck Converter for High Efficiency Wireless Power Transfer System", IEEE Trans. Industrial Informatics, Vol. 10, No. 3, pp. 1972–1980 (2014)

[10] J. Ito, K. Noguchi, and K. Orikawa: "Experimental Verification of Wireless Charging System for Vehicle Application using EDLCs", Proc. IECON 2014, pp. 1453–1459 (2014)

[11] T. Hiramatsu, H. Xiaoliang, M. Kato, T. Imura, and Y. Hori: "Wireless Charging Power Control for HESS through Receiver Side Voltage Control", Proc. APEC 2015, pp. 1614–1619 (2015)

[12] G. Yamamoto, T. Imura, and H. Fujimoto: "Maximizing Power Transfer Efficiency of Wireless In-wheel Motor by Primary and Load-Side Voltage Control", The 1st IEEJ International Workshop on Sensing, Actuation, and Motion Control, pp. 1–6 (2015)

[13] M. Kato, T. Imura, and Y. Hori: "New Characteristics Analysis Considering Transmission Distance and Load Variation in Wireless Power Transfer via Magnetic Resonant Coupling", Proc. INTELEC2012, pp. 1–5 (2012)

[14] T. Imura and Y. Hori: "Maximizing Air Gap and Efficiency of Magnetic Resonat Coupling for Wireless Power Transfer Using Equivalent Circuit and Neumann Formula", IEEE Trans. Industrial Electronics, Vol. 58, No. 10, pp. 4746–4752 (2011)